

# Experimental study of reinforced concrete pile caps with external, embedded and partially embedded socket with smooth interface

## *Estudo experimental de blocos de fundação com cálice externo, embutido e parcialmente embutido considerando interface lisa*



R. BARROS<sup>a</sup>  
barrosrn@sc.usp.br

J.S. GIONGO<sup>b</sup>  
jsgiongo@sc.usp.br

### Abstract

On Precast concrete structures the column foundation connections can occur through the socket foundation, which can be embedded, partially embedded or external, with socket walls over the pile caps. This paper presents an experimental study about two pile caps reinforced concrete with external, partially embedded and embedded socket submitted to central load, using 1:2 scaled models. In the analyzed models, the smooth interface between the socket walls and column was considered. The results are compared to a reference model that presents monolithic connections between the column and pile cap. It is observed that the ultimate load of pile cap with external sockets has the same magnitude as the reference pile cap, but the ultimate load of models with partially embedded and embedded socket present less magnitude than the reference model.

**Keywords:** reinforced concrete, pre cast concrete, pile caps, socket foundation.

### Resumo

Nas estruturas de concreto pré-moldado, a ligação pilar-fundação pode ocorrer por meio do cálice de fundação, que por sua vez pode estar embutido, parcialmente embutido com parte do colarinho saliente, ou externo com o colarinho saliente em relação ao bloco de fundação. Apresenta-se neste trabalho um estudo experimental de blocos de fundação sobre duas estacas com cálice externo, parcialmente embutido e embutido, submetidos à ação centrada utilizando modelos em escala reduzida 1:2. Nos modelos analisados, considerou-se a conformação lisa nas paredes do cálice e do pilar. Os resultados são comparados a um modelo de referência, com ligação monolítica entre o pilar e o bloco. Observa-se que o bloco com cálice externo apresenta força última com a mesma ordem de grandeza do bloco de referência, porém os blocos com cálice parcialmente embutido e embutido apresentam força última inferior a dos demais modelos.

**Palavras-chave:** concreto armado, concreto pré-moldado, blocos sobre estacas, cálice de fundação.

<sup>a</sup> Doutorando em Engenharia de Estruturas, Departamento de Engenharia de Estruturas, Escola de Engenharia de São Carlos, Universidade de São Paulo, barrosrn@sc.usp.br, Av. Trabalhador São Carlense, 400, CEP: 13566-590, São Carlos-SP, Brasil;

<sup>b</sup> Professor Doutor, Departamento de Engenharia de Estruturas, Escola de Engenharia de São Carlos, Universidade de São Paulo, jsgiongo@sc.usp.br, Av. Trabalhador São Carlense, 400, CEP: 13566-590, São Carlos-SP, Brasil.

## 1. Introduction

Pile caps are used in constructions whose foundations must reach the deep layers of the ground. In these situations, it is necessary to resort to the use of piles or large diameter bored piles. The connection between these elements and the superstructure is through the pile cap. On precast concrete structures, this connection can occur through the use of base plate, connection with reinforcement and grout, or socket. Amongst these types, the connection through socket is emphasized because it presents relative easy construction, adjustability and moment transmission from column to pile.

The socket is the part of the pile cap which receives the precast column, as a fit between these elements, and it may or may not have rough walls. The column remains in contact with the socket in a section called embedded length  $\ell_{emb}$ . In this type of connection, three socket situations are possible according to Figure 1: fully external with pedestal walls; partially embedded, where the embedded length is divided in external pedestal walls and embedded in the pile cap, or embedded in the pile cap, where there is no pedestal wall.

The theoretical models used to design pile caps are based on the bending theory when pile caps are thin, and on strut and tie models when the pile caps are thick. There are several studies on the design of socket base, amongst which the works of CANHA & EL DEBS [1] and CAMPOS et al [2] are emphasized.

Some studies show the development of strut and tie models which are used in designing monolithic connection pile caps. DELALIBERA & GIONGO [3] present a study on the influence of column cross section on the strut and tie models for two pile caps. SOUZA et al [4] present an adapted model considering an eccentricity in strut and tie models applied to four pile caps. BUTTIGNOL & ALMEIDA [5] developed a numerical study on three pile caps in which the characteristic value of compressive strength of concrete little influence on the load resistance of pile caps. However, there is little information in the technical literature regarding the structural behavior of pile caps with the presence of socket. BARROS [6] performed a numerical analysis in two pile caps with embedded socket considering the smooth and rough interface of socket walls.

For this reason, a theoretical and experimental research on pile caps considering the three possible socket scenarios was developed.

## 2. Method

The method applied in this research was the one commonly used to analyze theoretical and experimental studies on two pile caps. The results of the experimental tests on four pile caps in 1:2 scale are present in this paper. Three of the pile caps presented sockets, which were external, partially embedded and embedded. A smooth interface between the walls of the socket and the column was considered for all pile caps. A fourth block was analyzed, where the connection between the column and the pile cap occurred monolithically. This pile cap was nominated reference pile cap, and it was used for comparison with the results of pile caps with socket foundation.

### 2.1 Test specimens

The tests took place in the Structures Laboratory (LE) of the School of Engineering of Sao Carlos, University of Sao Paulo. All pile caps shared the same geometry plant, height (h) and pile spacing. Only the embedded length  $\ell_{emb}$  had influence on the distance  $h_{fund}$  from the bottom of the column to the bottom of the pile cap. In the case of the pile cap with the external socket, the distance  $h_{fund}$  coincided with the height of the pile cap. In the pile cap with partially embedded socket, half of the embedded length  $\ell_{emb}$  was external to the pile cap and the remaining length was inside the pile cap. In the pile caps with embedded socket, full length  $\ell_{emb}$  was within the pile cap. The four models analyzed were named M1, M2, M4 and M6, as shown in Table 1.

### 2.2 Model design

The design of the pile caps was made from a monolithic pile cap in real scale with square columns and piles, and its edges measured 30 cm. The height of the pile caps was defined considering the minimum embedded length  $\ell_{emb\ recommended}$  by ABNT NBR 9062:2006 [7] for normal force with small eccentricity, and design based on

Figure 1 – Pile caps with external, embedded and partially embedded socket

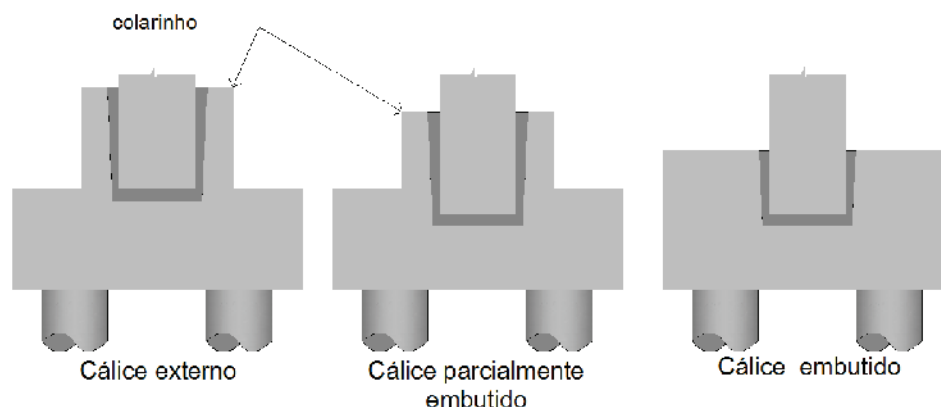


Table 1 – Analyzed models in laboratory

Socket type	Model	$h_{fund}$
Reference	M1	h
External	M2	h
Partially embedded	M4	$h - (\ell_{emb}/2)$
Embedded	M6	$h - \ell_{emb}$

the recommendations of ABNT NBR 6118:2007 [8] and BLÉVOT & FREMY [9]. The inclination of the strut has been taken from a line segment connecting the center of the pile to the center of half of the column area for each of the piles. Figure 2 illustrates the dimensions of the pile cap in real scale.

To obtain the theoretical load supported by the pile cap, the limit stress values on nodal zones were used as limiting values, that is, at the intersection of the strut and the column and the strut and the pile. Because of the design of elements that were scientifically tested, the load safety factor value,  $\gamma_f = 1$  was used, considering the theoretical force as evaluation Load,  $F_{ava}$ . Regarding the limit stress value on nodal zones, the stress safety factor values indicated in standards were not decreased, and the value of the characteristic resistance to compression of the concrete  $f_{ck}$  was adopted, according to equation 1.

$$F_{ava} = f_{ck} \cdot A_p \cdot \sin^2 49,2 = 0,57 \cdot f_{ck} \cdot A_p \quad (1)$$

Because the piles and the columns have the same area, the limiting condition for the design is the stress on the intersection of the strut and the column. Common concrete with characteristic resistance to compression  $f_{ck} = 25$  MPa was used. The calculation of the strength on the tie is done by balancing the triangle of strength on the intersection of the strut and the pile, and the  $R_{st}$  strength is obtained from the ratio between the tangent of strut angle inclination and the strength on this strut. The calculation of the required reinforcement is obtained from the relation of strength on the tie  $R_{st}$  and yield stress of reinforcement bars  $f_{yk}$ . For the same reasons previously admitted for the concrete, the coefficient of decreasing resistance  $g_s = 1$  for steel was adopted. Since reduced models maintain the 1:2 scale, the design of these models is done by changing the geometry of the pile caps, resulting in the values presented below:

$$F_{ava} = 0,57 \cdot 2,5 \cdot 15 \cdot 15 = 320,625 \text{ kN} \quad (2)$$

$$R_{st} = \frac{320,625}{2 \cdot \text{tg}49,2} = 138,3 \text{ kN} \quad (3)$$

$$A_{st} = \frac{138,3}{50} = 2,77 \text{ cm}^2 \quad (4)$$

Therefore, the main reinforcement of the pile cap was detailed with 4f8.0 mm e 1f10.0 mm totaling 2.78 cm<sup>2</sup>. The rate of steel was kept constant in all four pile caps, so that this parameter does not directly interfere in the comparison of the models results. The design of columns and piles was applied according to the recommendations of ABNT NBR 6118:2007 [8] with the consideration of minimum moment applied to these elements, resulting in 4f10.0 mm for the piles and 4f12.5 mm for the columns. Regarding the design of socket, the recommendations of small eccentricity were considered, since the experiments were performed under the action of centered load applied to the column, resulting in minimal reinforcement when CA-60 steel bars with a 5.0 mm diameter were used.

### 3. Experimental program

#### 3.1 Molds

The molds of pile caps, columns and piles were made with plasticized plywood of 17 mm thickness in the joinery of EESC-USP. Besides plywood, rafters were used for lateral restraint of molds, nails, screws and glue. Figure 3 shows the mold of the external socket and the mold of one of the pile caps with the piles placed before concreting.

#### 3.2 Reinforcement bars

CA-50 steel bars with diameters of 6.3 mm, 8.0 mm, 10.0 mm and 12.5 mm and CA-60 steel bars with nominal diameter of 5.0 mm were used. It was necessary to assemble the reinforcement bars, which occurred in the LE (Structures Laboratory). The assembly sequence begins with piles, since they didn't present strain gauges

Figure 2 – Dimensions of real scale model

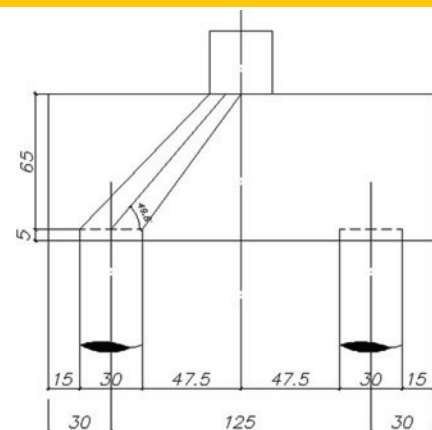


Figure 3 – External socket and pile caps molds



in their bars. Then the reinforcement bars of the columns were assembled, and finally, the reinforcement bars of pile caps along with the sockets. Figure 4 shows the stage of design and the reinforcement bars of the columns after assembly, and figure 5 shows the assembly of the reinforcement bars of the pile cap.

### 3.3 Molding

The piles were molded first, because they had to be placed in the mold before the pile cap concreting. The pile caps and the socket walls were cemented later and, lastly, the columns. The compressive strength of the concrete used for columns and piles was higher than the pile caps resistance. Class C50

concrete was used for the columns and piles, and class C25 concrete was used for pile caps and sockets. The difference in the resistance of the elements was intended to prevent the ruin of the models in the piles or columns. The class C50 concrete was made in the laboratory of structures (LE) while the class C25 concrete was purchased from a supplier of ready-mixed concrete.

The dosage used to prepare the class C50 concrete was established according to AITCIN [10]. The dosage used for the columns and piles was 1:2,36:2,54:0,33:0,03 (cement, sand, crushed stone, a/c superplasticizer Glenium 51, chloride-free). Were used high initial resistance cement CPV-ARI. The thin aggregate used was quartz sand available in the region of Sao

Figure 4 – Details of column reinforcement bars

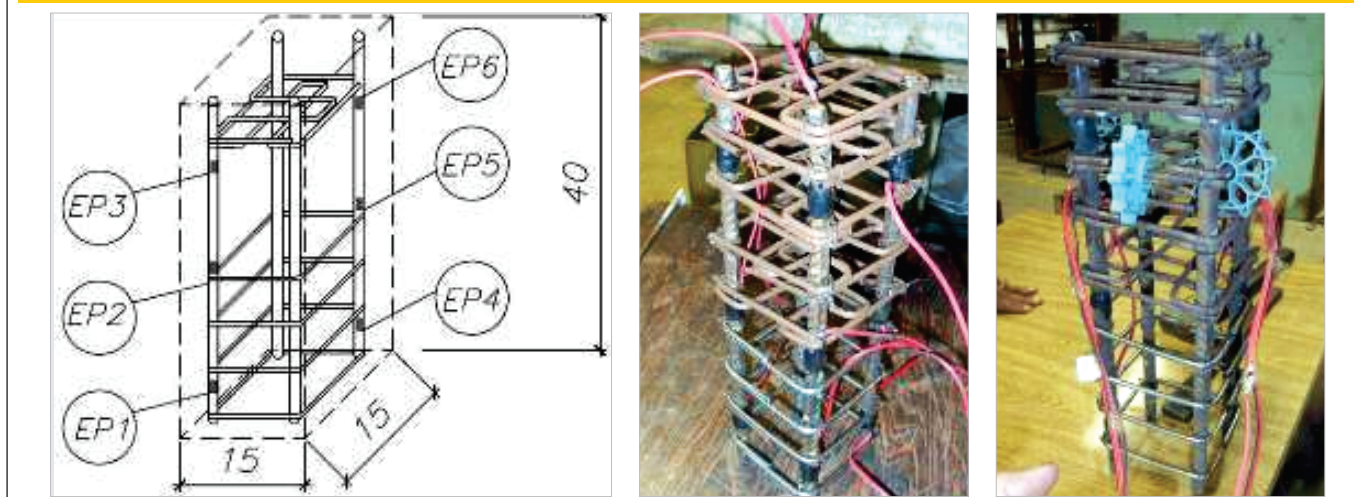


Figure 5 – Details of socket and pile caps reinforcement bars



Carlos. The thick aggregate was crushed basaltic rock with a maximum diameter of 19 mm. The water used in the dosages was provided by the public water supply of the city of Sao Carlos, and the superplasticizer used was obtained through donation.

Plastic spacer blocks were used to position the reinforcement bars in the pile cap molds, so as to ensure a minimum coating of 2.50 cm for the reinforcement. The tips of the strain gauges wires were wrapped with plastic to prevent damage caused by fresh concrete. Figure 6 shows the model M2 pile cap before and after casting.

The column concreting occurred after the pile caps concreting. As stated earlier, the concrete used in the columns was the same used in the piles. The precast columns were molded

separately and placed in the socket pile caps. The column of the reference pile cap was molded directly onto the pile cap.

After all the elements were unmolded, it was necessary to connect the columns and the pile caps. This connection was made by positioning the columns within the socket foundation. Firstly, the sockets were cleaned and the dust that had accumulated inside of them was removed, and the socket walls were cleaned with a damp cloth. After cleaning, the positioning of the precast columns was made.

For the positioning, it was necessary to check the level and plumb of the columns in relation to the surface. Then the space between the columns and the sockets was filled with self-compacting grout. The grout presents dried density equal to 2.28 g/cm<sup>3</sup>, workability time of 30 minutes and an estimated consumption of 2000 kg/m<sup>3</sup>.

Figure 6 – Concrete casting of pile caps



Figure 7 – Positioning of column in socket foundation and grout filling



Figure 7 illustrates the positioning of the column and the filling of the grout.

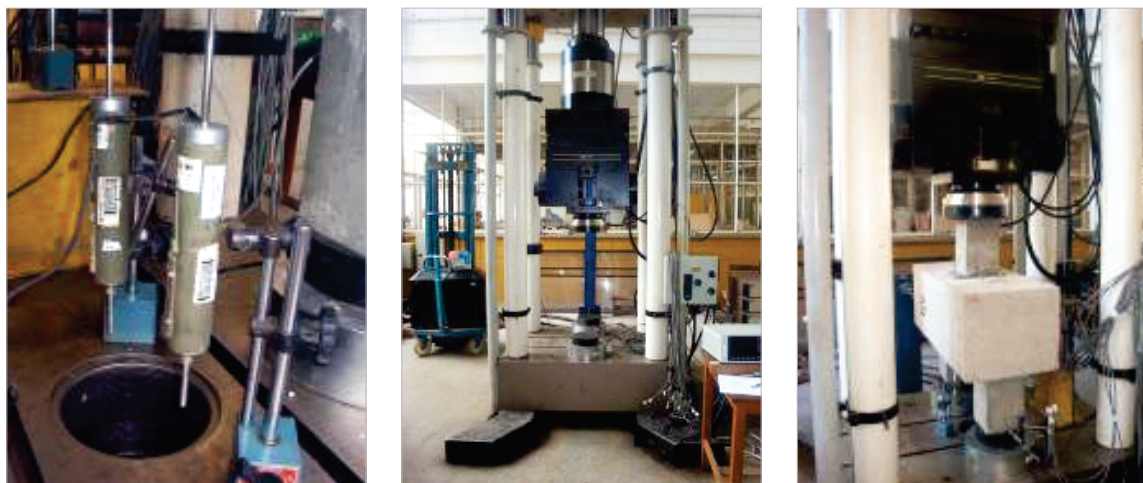
### 3.4 Equipment and instrumentation

The tests were performed at the Laboratory of Structures of EESC-USP, using the universal servo-controlled testing machine Instron 8506, with a nominal load capacity equal to 2500 kN. This equipment was also utilized for the characterization tests of steel reinforcement bars. For automatic retrieval of data on measures of strain and displacement obtained with electrical-resistance strain gauges and displacement transducers, the System 5000 was used. The mechanical properties of concrete, steel and grout were obtained from characterization tests. For the tests of concrete pile

caps, columns and piles, cylindrical specimens measuring 10 cm in diameter and 20 cm in height were used. For the tests of grout, cylindrical specimens measuring 5 cm in diameter and 10 cm in height were used. These tests followed the recommendations of ABNT NBR 5738:2008 [11] ABNT NBR 5739:2007 [12] and ABNT NBR 7222:2011 [13].

The measures of strain of the models reinforcement bars were obtained by Kyowa uniaxial electrical-resistance strain gauges, with measure base of 5 mm and strain gauge factor equal to 2.10, which were glued to the reinforcement bars of pile caps and columns. Main tie reinforcement bars were instrumented in all pile caps. These strain gauges were positioned in three specific sections, two of which are positioned on the geometric center of the piles and the other in the central region of the pile caps.

Figure 8 – Universal Instron machine 8506 used on tests



The reinforcement of the precast columns was instrumented in two longitudinal bars with three strain gauges on each bar, totaling six strain gauges for each column. The purpose of using these strain gauges was to check, by means of strain measurement, if the load from the column was transferred to the pile cap along the column embedded length or if the load transfer occurred directly through the inferior region of the column.

Measurements of displacement in the models were obtained by the use of displacement transducers with measurement of 50 mm and positioned in the inferior region of the pile cap to measure vertical displacement. Figure 8 shows the displacement transducers and the Instron universal machine 8506 with the pile cap prepared for the test.

## 4. Results

### 4.1 Materials properties

In this section, the results of the mechanical properties of the materials used in the construction of models are presented. For the grout and concrete used in the models, the results of average compressive strength ( $f_{c,m}$ ), tensile strength by average diametral compressive test ( $f_{t,m}$ ), average axial tensile strength ( $f_{ct,m}$ ) and initial average tangent modulus of elasticity ( $E_{ci,exp,m}$ ) – which were obtained from the average of the results of four specimens – are presented in Table 2.

Regarding the reinforcement steel bars, values of simple tensile strength and modulus of elasticity were obtained, and three bars were used for each diameter. To determine the modulus of elasticity of the steel bars, the straight segment of the stress-strain curves obtained experimentally was used. The modulus of elasticity of the steel bars CA-50 resulted in an average value of 203 GPa, while the average strain from which the yield started ( $\epsilon_{ym}$ ) was 2.81 ‰, corresponding to an average yield stress equal to 569 MPa.

After the materials characterization tests it was necessary to correct the value of the evaluation load in order to compare the predicted value in the theoretical model with the value experimentally obtained. When the value  $f_{ck}$  in equation 1 is replaced for the value of  $f_{cm}$ , it is possible to obtain a new value for the evaluation load, however, the steel area exceeds the steel area detailed in the models.

It was possible to calculate a new evaluation load from the values of  $f_{cm}$  and  $f_{ym}$ , resulting in a steel area which is equal to the one predicted in the detailed models. In this situation, it is clear that both the evaluation load and the stress on the tie are functions of

the angle  $\theta$  of inclination of the strut. This situation is possible, considering that the tests performed showed an increase in the load applied to the pile cap even after the yield of the main reinforcement bars of the tie. From the expressions (1) and (2), the detailed reinforcement area and materials strength values, one obtains the equations (5) and (6).

$$F_{ava} = f_{cm} \cdot A_p \cdot \text{sen}^2 \theta = 3,3 \cdot 15 \cdot 15 \cdot \text{sen}^2 \theta = 742,5 \cdot \text{sen}^2 \theta \quad (5)$$

$$F_{ava} = 158,2 \cdot 2 \cdot \text{tg} \theta = 316,4 \cdot \text{tg} \theta \quad (6)$$

Relating these equations with the trigonometric general equation, which considers the sine and cosine of an angle, one obtains an equation of the second degree, in which one of the roots is the angle  $\theta$  equal to 60.8 °, resulting in an evaluation load equal to 565 kN.

### 4.2 Reference pile cap

The M1 model presented rigid pile cap behavior according to the theoretical model considered. A small eccentricity in the load applied on the 1.65 cm column was recorded. The ruin of the model was due to the yield of all the main reinforcement bars of the tie, located in the central region of the pile cap.

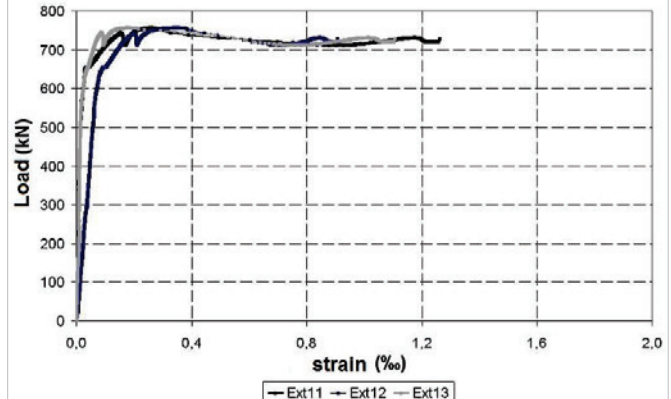
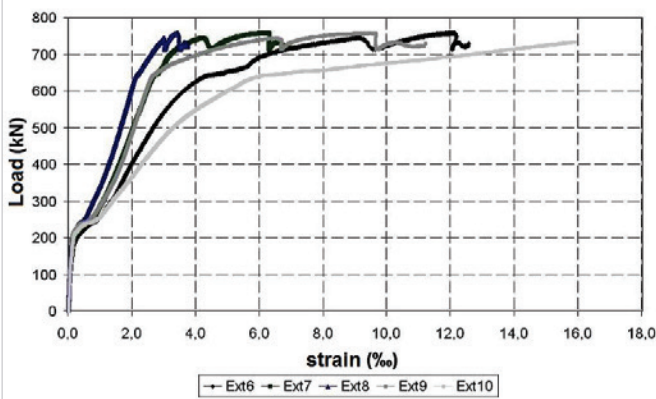
The maximum load recorded for this model was 756 kN, which is higher than the calculated load in the theoretical model used for design. The model showed increasing strength until it reached 743 kN, and then there was a small decrease in its value. However, it showed increasing load again, until it ruined at 756 kN. The first visible crack in the model presented an opening of 0.05 mm, which occurred in the inferior lateral face of the pile cap when considering a load on the column equal to 230 kN. In this step, the maximum strain of the five reinforcement bars in the tie was 0.596 ‰, resulting in a tensile strength of 119 MPa. It was observed that the model had decrease of stiffness at approximately 210 kN.

Figure 9 shows a graph representing load *versus* mean strain of the reinforcement bars positioned in the central region of the pile cap and a graph representing the load-strain of the reinforcement bars placed on piles. It is observed through these graphs that the strain in the reinforcement over the piles present low values when compared to the strains measured in the reinforcement in the central region of the pile cap. This is due to the formation of the strut on the piles, which causes a decrease in the strength of the tie in this region. As the load on the piston increased, the emergence of new cracks and an increase in the opening of existing cracks were verified. It was verified that crack openings of 0.1 mm, 0.25 mm and 0.8 mm correspond to loads of 360 kN, 660 kN and 720 kN, respectively. The cracks that began in central region of the pile cap continued until the upper region, forming two visible crack planes, dividing the pile cap into three distinct parts.

**Table 2 – Results of mechanical properties of materials**

Element	$f_{c,m}$ (MPa)	$f_{t,m}$ (MPa)	$f_{ct,m}$ (MPa)	$E_{ci,exp,m}$ (GPa)
Column	37,7	3,09	2,78	30,05
Pile	70,5	4,89	4,40	42,9
Grout	64,2	3,56	3,20	41,8
Pile cap	33,1	2,47	2,22	25,2

Figure 9 - Load-strain curve on reinforcement bars positioned in central region and over piles



### 4.3 Pile cap with external socket

The M2 model showed a small eccentricity in the applied load on the 1.38 cm column. The ruin of the model was due to the yield of all the main reinforcement bars of the tie, located in the central region of the pile cap.

The maximum load supported by this model was 772 kN, which is higher than the calculated load in the theoretical model used for design. The model presented increasing strength until it reached a load of 690 kN, and then there was a decrease in its value up to 650 kN. Afterwards, the pile cap showed increasing load again, until it ruined at 772 kN. It is observed that the ultimate value of force in model M2 was close to the value of 756 kN obtained in the reference pile cap M1.

The first visible crack in model M2 appeared in the upper region of the pile cap near the socket, at a load of 100 kN. Then, crack openings of 0.05 mm occurred in the inferior central region of the pile cap, at a load on the column of 320 kN. In this step, the maximum

strain of the five reinforcement bars in the tie was 0.38 ‰, resulting in a tensile strength equal to 77 MPa. It was observed that the model presented stiffness loss at a load close to 310 kN, as seen in the graphs of load-strain of the reinforcement bars positioned in the central region of the pile cap

Figure 10 shows the graph load *versus* mean strain related to the reinforcement bars positioned in the central region of the pile cap for models M1 and M2, and the curve load-strain in the reinforcement positioned along the column. It is observed through this figure that the pile cap with external socket was stiffer than the reference pile cap, and that the strain of the reinforcement bars of the columns became smaller as the column is near the bottom of the socket. However, this decrease is small, indicating that despite the fact that the compression strut is formed along the height of the socket, part of the load is transmitted directly to the bottom of the socket.

Openings of cracks of 0.15 mm, 0.25 mm and 0.3 mm correspond to loads of 420 kN, 500 kN and 620 kN, respectively. There were four crack lines in the central region of the pile cap, which contin-

Figure 10 - Load-strain curve on reinforcement bars positioned in central region and along column of model M2

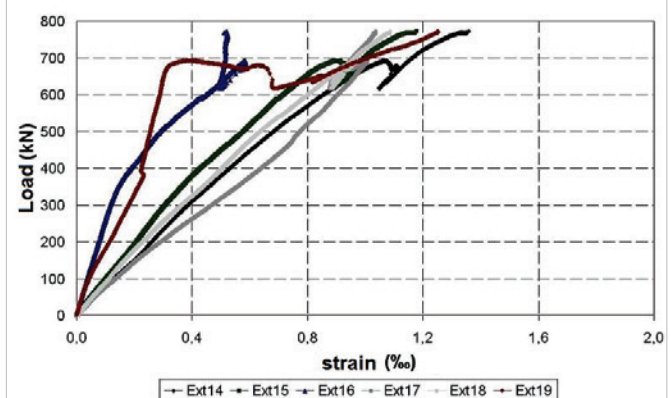
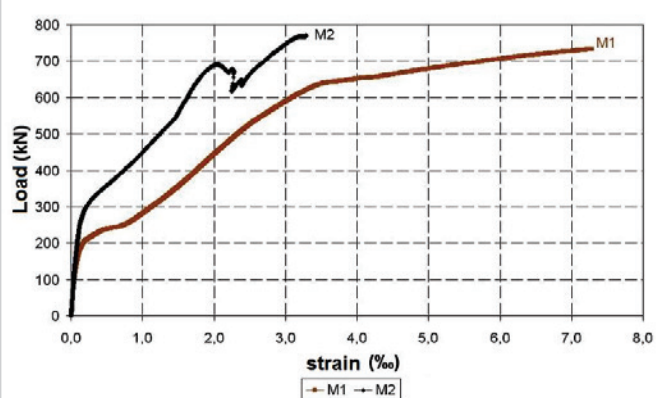


Figure 11 – Cracking overview of models M1 e M2



ued until the upper region. It was also observed the formation of horizontal cracks in the region of the socket at loads near the ruin of the model. Figure 11 shows the overview cracking from M1 and M2 models.

#### 4.4 Pile caps with partially embedded socket

The M4 model recorded an eccentricity in the load applied to the column of 1.17 cm. The ruin of the model was due to the yield of all the main reinforcement bars of the tie, located in the central region of the pile cap, followed by rupture of the pile cap concrete.

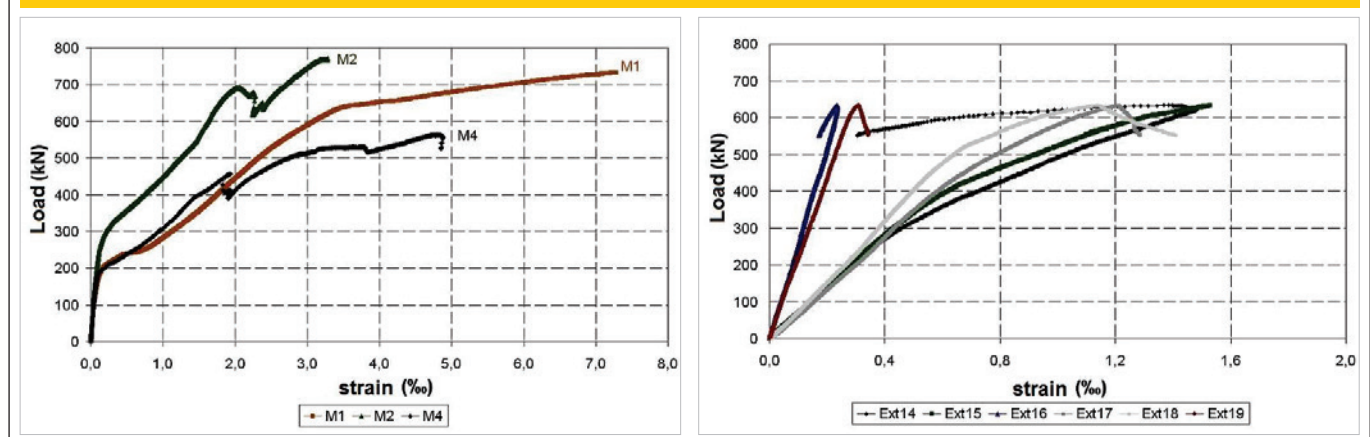
The maximum load supported by this model was 563 kN, which was higher than the load calculated with the theoretical model used for design. The model showed increasing resistance until reaching a force of 460 kN, with two large cracks in the central region, where

there was a decrease in resistance at 400 kN. Then the pile cap showed increasing strength, until the ruin at 563 kN. It is observed that the value of the ultimate strength of the M4 model was lower than the value of 756 kN obtained in the reference pile cap, as well as the ultimate strength obtained in the M2 model.

The first visible crack in the M4 model appeared in the inferior central region of the pile cap, with an opening of 0.05 mm for a load of 210 kN. In this step, the maximum strain measured on the reinforcement bars of the tie was 0.26 ‰ which results in a tensile strength of 53 MPa. It was observed that the model had decrease of stiffness at a load close to 190 kN, as it can be observed in the load-strain graphs of the reinforcement bars positioned in the central region of the pile cap.

Figure 12 shows the load *versus* mean strain graph in relation to the reinforcement bars positioned in the central region of the pile

Figure 12 – Load-strain curve on reinforcement bars positioned in central region and along column of model M4



cap for models M1, M2 and M4, and the load-strain curve in the reinforcement bars positioned along the column. It is observed through this figure that the M4 model presented stiffness similar to the reference pile cap when submitted to a load up to 450 kN, and less stiffness than the M2 model pile cap with external socket. It is also observed that, when submitted to a load of 450 kN, the M4 model presented medium strain in the reinforcement bars, which was higher than those obtained in models M1 and M2. In light of these results, it is clear that the formation of the compression strut in the M4 model presents inferior inclination of the tie when compared to the reference pile cap inclination.

As in the M2 model, there is less strain of the columns reinforcement bars when the column is near the bottom of the socket. However, part of the column force was directly transmitted to the bottom of the socket.

The M4 model presented openings of about 0.15 mm, 0.25 mm and 0.30 mm corresponding to loads of 310 kN, 380 kN and 440 kN, respectively. After the M4 model presented a decrease in strength,

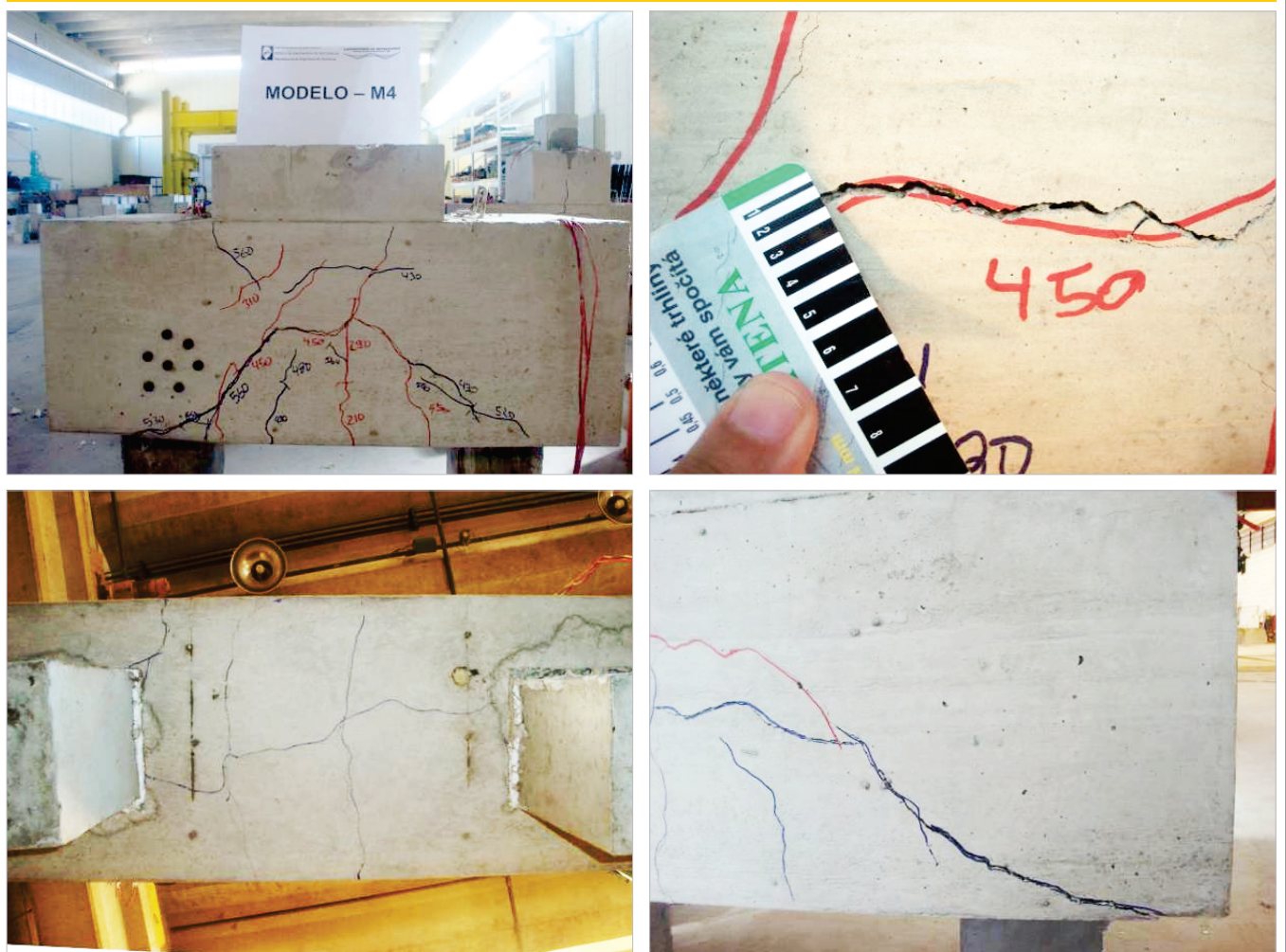
as previously mentioned, an increase in crack openings – with maximum openings of approximately 2.00 mm – was observed. Figure 13 presents a cracking overview of the M4 model after the tests.

Cracks were noted in the central region of the pile cap. One of the cracks extended through the inferior region of the pile cap and appeared on the opposite side, causing separation of the pile caps concrete. It was also observed the formation of cracks in the inferior region of the pile cap and there was no cracking through the pile cap towards the pedestal walls, at the top of the socket.

#### 4.5 Pile caps with embedded socket

The M6 model behaved as a flexible pile cap. A small eccentricity in load applied on the column of 0.09 cm was recorded, setting up a situation in which there is centered load. The ruin of the model was due to the yield of the main reinforcement bars of the tie located in the central region of the pile cap, and the rupture of concrete of pile cap did not occurred.

Figure 13 – Cracking overview of model M4



The maximum load supported by this model was 359 kN, which is similar to the load calculated with the theoretical model used for design. The model showed increasing resistance until reaching the ultimate load of 359 kN, with a single vertical crack that extended to the top of the pile cap, and several horizontal cracks which extended throughout the inferior region of the pile cap. It is observed that the value of the ultimate strength of the M6 model was lower than the maximum value of 756 kN obtained in the reference pile cap. The strength of this model was also lower than the M2 model, which presented external socket, and the M4 model, which presented partially embedded socket.

The first visible crack in the M6 model appeared in the central inferior region of the pile cap, with an opening of about 0.05 mm at a load of 170 kN. In this step, the maximum strain measured on the reinforcement bars of the tie was 0.28 ‰, which results in stress equal to 57 MPa. It was observed that the model presented stiffness loss at a load close to 160 kN, as it can be seen in the graphs of load-strain of the reinforcement bars positioned in the central region of the pile cap.

Figure 14 shows the graph of load *versus* mean strain in relation to the reinforcement bars positioned in the central region of the pile cap for models M1, M2, M4 and M6, and the curve load-strain in the reinforcement bars positioned along the column. It is observed through this figure that the M6 model presented less stiffness than the models analyzed, and it presented more strain in the main reinforcement bars of the tie than the other models. Comparing the M6 model to the reference pile cap, a reduction of 40% in the load acting on the column is stated for an average strain in the reinforcement bars close to 3.8 ‰. Based on the results presented, it is clear that there was no formation of compression struts in the M6 model, which presented a flexible pile cap behavior.

It was verified that crack openings of about 0.15 mm, 0.20 mm, 0.30 mm and 0.50 mm correspond to loads of 200 kN, 230 kN, 260 kN and 320 kN, respectively. It was also verified that there was an increase of the crack openings near the ruin of the model, and horizontal openings up to 2.00 mm appeared. There were several cracks in the central region of the pile cap, and some of these cracks extended through the inferior region of the pile cap

and emerged on the other side. Figure 15 provides an overview of the cracking and concrete detachment located in the inferior region of the pile cap.

#### 4.6 Results analysis

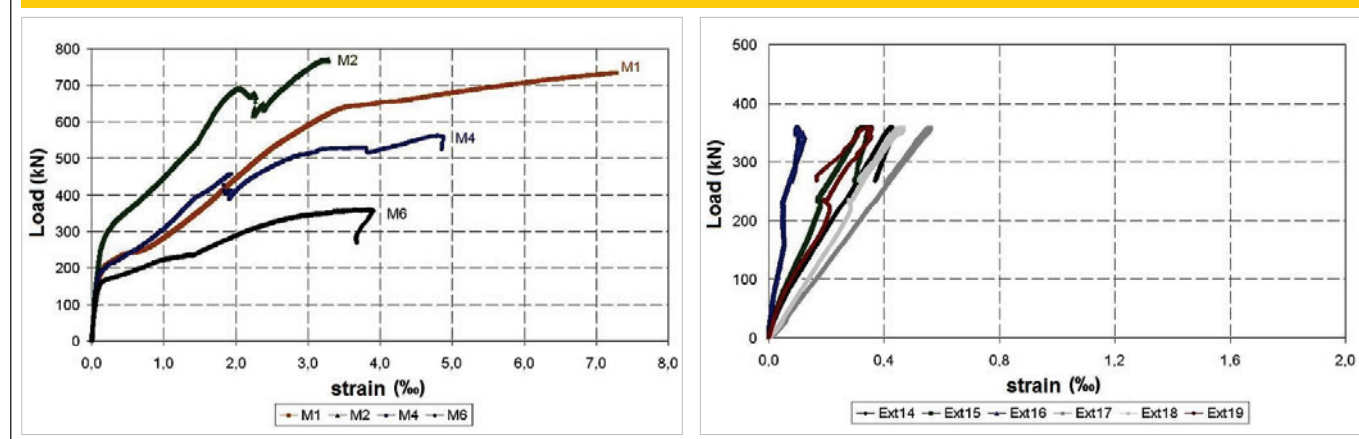
Regarding the ultimate strength of the models, it is verified that only the pile cap with external socket presented ultimate strength up to 2% higher than that of the reference pile cap. Pile caps with partially embedded and embedded socket presented less ultimate load than the reference pile cap, with values of 74% for the M4 model and 47% for the M6 model in relation to the ultimate load of the reference pile cap.

Regarding the evaluation load, it was verified that only the pile cap with embedded socket with smooth interface presented experimental load inferior to the theoretical strength, indicating that the calculation procedure used in the design of these pile caps is not proper to meet security regulations. The pile cap with partially embedded socket presented ultimate strength equal to the theoretical evaluation strength, while the pile caps with external socket and the reference pile cap presented ultimate strength superior to the theoretical strength. These relations are shown in table 3.

Regarding the transfer of forces from the column to the socket through the instrumentation of the column reinforcement, measures of strain of these bars were obtained. Using the value of the modulus of elasticity of the steel bars obtained through material characterization it was possible to estimate the force acting on the reinforcement bars of the columns arranged in three sections along the length of the column. Section S1 was positioned near the top of the column; section S2 was positioned in the central region of the column and section S3 was positioned in the inferior region of the column.

Because of the small eccentricities registered in the models, it was verified that the stress distribution in the column occurred uniformly. It was simply assumed that the strain in the four reinforcement bars of the column was equal to the average value obtained in the two strain gauges positioned in the reinforcement bars in each section. Considering the perfect bonding between the concrete

Figure 14 – Load-strain curve on reinforcement bars positioned in central region and along column of model M6



and the reinforcement bars, it can be assumed that the strain in the concrete is very close to the strain of the steel bars. From the stress-strain curve obtained in the characterization tests of the columns concrete, the mean compressive stress acting on the column concrete is obtained, with which one obtains the portion of load on concrete. By joining the portions of load of the reinforcement bars and the column concrete, it is possible to establish a theoretical force value acting on the column,  $F_{teo,p}$  obtained with the experimental data, using expression 7.

$$F_{teo,p} = \epsilon_s \cdot E_s \cdot A_s + f_c \cdot A_c \quad (7)$$

Using the strain data obtained in section S1 on the imminence of the ruin of the models, it is possible to compare the theoretical force on the column to the ultimate load value in models, which

**Table 3 – Relation between ultimate load and evaluation load**

Model	$F_u$ (kN)	$F_{,ava}$ (kN)	$F_u/F_{,ava}$ (%)
M1	756	565	134
M2	772	565	137
M4	563	565	100
M6	359	565	64

was recorded in the test step. Differences in the order of 10% between the theoretical and the experimental value were verified, and are disposed in table 4.

Because it is a model of calculation, there are differences between the forces values recorded in the test and those predicted in the

**Figure 15 – Cracking overview of model M6**

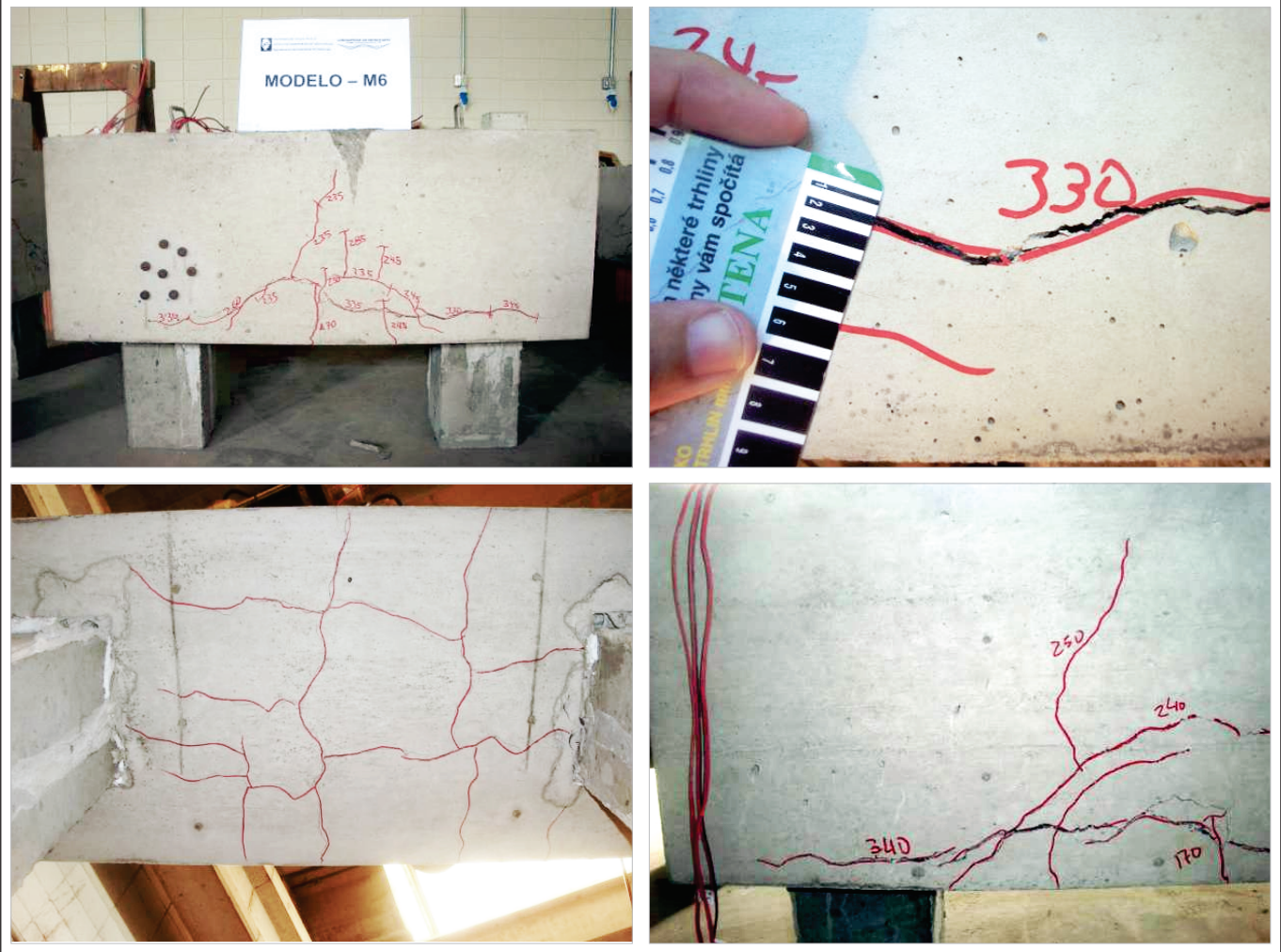


Table 4 – Theoretical ultimate load on column

Model	$\varepsilon_{s,S1}$ (‰)	$f_c$ (MPa)	$F_{reint}$ (kN)	$F_{concrete}$ (kN)	$F_{theo,c}$ (kN)	$F_u$ (kN)	$F_{theo,c}/F_u$ (%)
M2	1,20	26,9	116,0	591,8	707,8	772	92%
M4	1,00	24,0	94,9	528,0	622,9	563	111%
M6	0,50	14,0	47,7	308,0	355,7	359	99%

theoretical model. These differences can be attributed to the following factors: regions in which slip of reinforcement bars may have occurred and where there is no perfect bonding between concrete and reinforcement; non-uniform distribution of stresses in the cross section due to recorded small eccentricities; and average values of steel and concrete resistance obtained from tests of characterization.

As in section S1, the calculation of forces acting on the concrete and reinforcement bars in sections S2 and S3 was made, and these sections were located in the middle and in the inferior region of the column, respectively. Thus, it was possible to analyze the evolution of strength in these sections as well as the transfer of strength from the column to the pile cap. It was verified that there is a reduction of the force acting on section S1 to S3 section, that is, the dissipation of the column strength occurs as it is in contact with the socket. It was found that the pile caps in section S3 present an average force equivalent to 55% of the force acting on section S1, that is, 55% of the force acting on the column is transmitted to the pile cap directly from the bottom of the socket, as shown in Figure 16.

## 5. Conclusion

Through the results obtained from laboratory tests it was verified that the pile cap with external socket presented ultimate strength similar to the one obtained from the reference pile cap with monolithic connection, while the pile caps with partially embedded and embedded socket presented less ultimate strength than the reference pile cap.

Regarding the evaluation load, it was found that the pile cap with embedded socket presented less ultimate strength than the evaluation load recorded after the materials characterization, indicating that the theoretical model used for design of this type of pile cap does not meet safety regulations.

Regarding the strains measured on the reinforcement bars of the columns, it was found that the transfer of strength from the column to the pile cap occurs partly because of the formation of the compression strut along the socket, and partly because of direct transmission to the bottom of the socket. Further tests considering the existence of roughness on the interface between the column and the socket are recommended.

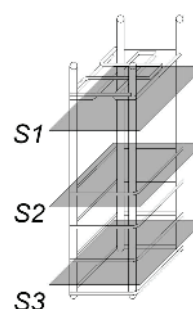
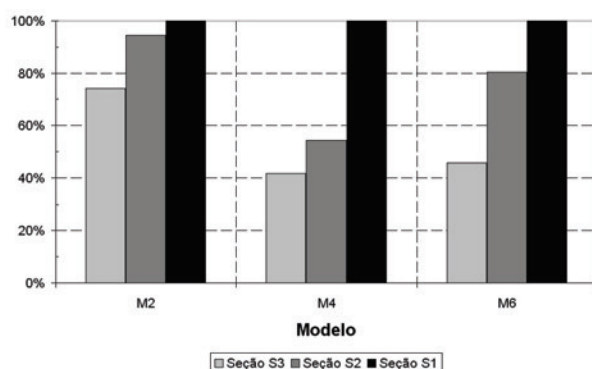
## 6. Acknowledgements

The authors thank the staff from the Structures Laboratory at the Department of Structural Engineering of Sao Carlos Engineering School, University of São Paulo, and CNPq for the PhD scholarship granted to the first author.

## 7. References

- [01] CANHA, R. M. F.; EL DEBS, M. K. Critical analysis of models and recommendations for designing column-base connection by socket of precast concrete structures. IBRACON Structural Journal, v.2, n.2, p.116-136, June.2006.
- [02] CAMPOS, G. M.; CANHA, R. M. F.; EL DEBS, M. K. Design of precast columns bases embedded in

Figure 16 – Transfer diagram of load from column to pile caps



- socket foundations with smooth interfaces. IBRACON Structural and Material Journal, v.4, n.2, p.314-323, June.2011.
- [03] DELALIBERA, R. G.; GIONGO, J. S. Influence of column cross section and eccentricity of compression load in structural behavior of two pile caps. IBRACON Structural and Material Journal, v.2, n.4, p.306-325, December.2009.
- [04] SOUZA, R. A.; KUCHMA, D. A., PARK, J.; BITTENCOURT, T. N. Adaptable strut-and-tie model for the design and verification of four pile caps. ACI Structural Journal. v. 106, p. 1-9, 2009.
- [05] BUTTIGNOL, T. E. T.; ALMEIDA, L. C. Concrete compressive characteristic strength analysis of pile caps with three piles. IBRACON Structural and Material Journal, v.6, n.1, p.158-177, February. 2013.
- [06] BARROS, R. Análise de blocos de concreto armado sobre duas estacas com cálice totalmente embutido mediante presença de viga de travamento. Dissertação (Mestrado), Escola de Engenharia de São Carlos, Universidade de São Paulo, São Carlos. 2009.
- [07] ASSOCIAÇÃO BRASILEIRA DE NORMAS TÉCNICAS. NBR 9062 – Projeto e execução de estruturas de concreto pré-moldado. Rio de Janeiro, ABNT. 2006
- [08] ASSOCIAÇÃO BRASILEIRA DE NORMAS TÉCNICAS. NBR 6118: Projeto de estruturas de concreto – Procedimento. Rio de Janeiro, 2007.
- [09] BLÉVOT, J.; FRÉMY, R. Semelles sur pieux. Anales d'Institut Technique du Bâtiment et des Travaux Publics, Paris, v. 20, n. 230, 1967, p. 223-295, fev;
- [10] AITCIN, P. C. Concreto de alto desempenho, 1 ed. P. 667. São Paulo,2000;
- [11] ASSOCIAÇÃO BRASILEIRA DE NORMAS TÉCNICAS. NBR 5738: Procedimento para moldagem e cura de corpos-de-prova de concreto. Rio de Janeiro, 2008.
- [12] ASSOCIAÇÃO BRASILEIRA DE NORMAS TÉCNICAS. NBR 5739: Concreto - Ensaios de compressão de corpos-de-prova cilíndricos. Rio de Janeiro, 2007.
- [13] ASSOCIAÇÃO BRASILEIRA DE NORMAS TÉCNICAS. NBR 7222: Concreto e argamassa — Determinação da resistência à tração por compressão diametral de corpos de prova cilíndricos. Rio de Janeiro, 2011.